Laser and Particle Beams (2013), *31*, 163–169.

doi:10.1017/S0263034612000985

Third harmonic generation of a nonlinear laser Eigen mode of a self sustained plasma channel

K.K. MAGESH KUMAR AND V.K. TRIPATHI
Physics Department, Indian Institute of Technology Delhi, New Delhi, India
(RECEIVED 18 July 2012; ACCEPTED 17 October 2012)

Abstract

The third harmonic generation of a self organized nonlinear laser Eigen mode of a two-dimensional plasma channel with complete electron evacuation from the inner region is investigated. The nonlinearities arise through the ponderomotive force and relativistic mass variations, while the ions are taken to be immobile. The second harmonic ponderomotive force produces electron density oscillations that beat with the oscillatory velocity due to the laser Eigen mode to create a nonlinear current, driving the third harmonic. As a_0 increases up to the threshold value $a_{\min}$, at which complete electron evacuation begins in the inner region, the third harmonic amplitude rises rapidly. Above the threshold, as a_0 increases, the width of the inner region where there is no third harmonic current, increases and third harmonic amplitude rises less rapidly. The conversion efficiency is found to be in reasonable agreement with the experimental results.

Keywords: Eigen mode; Electron density oscillations; Ponderomotive force; Sustained plasma channel; Third harmonic generation

1. INTRODUCTION

Ultrahigh intensity laser plasma interaction has evolved several novel concept and applications, such as, laser-driven electron accelerators (Tajima & Dawson., 1979; Sprangle *et al*., 1988; Modena *et al*., 1995; Ting *et al*., 1997), X-ray lasers (Burnett & Enright, 1990), fast ignitor inertial confinement fusion (Tabak *et al*., 1994), ion Coulomb explosion, etc. These applications require long laser propagation distances, in excess of Rayleigh length. Various mechanisms have been demonstrated for the guiding of intense laser pulses in plasmas (Kumarappan *et al*., 2005; Geddes *et al*., 2005; Malka *et al*., 1995; Nikitin *et al*., 1997; Sprangle *et al*., 1992; Verma & Sharma, 2009*a*; 2009*b*; Singh & Singh, 2011). A Laser of intensity 5×10^{15} W/cm^2 has been channeled up to 3 cm in a preformed plasma waveguide structure created by the hydrodynamic expansion (Durfee & Milchberg, 1993). Jackel *et al*. (1995) guided laser pulse of intensity 10^{16} W/cm^2 using glass capillary waveguides in vacuum and Ehrlich *et al*. (1996) used long cylindrical plasma channel formed by a slow capillary discharge. More detailed analyses of self-focusing and channeling of a short relativistic laser pulse has been done by various groups (Sprangle *et al*., 1992; Bulanov *et al*., 1995; Mora & Antonsen, 1996; Sarkisov *et al*., 1996; Borisov *et al*., 1992).

Sun *et al*. (1987) and Borisov *et al*. (1992) have studied the nonlinear propagation of intense ultrashort cylindrically symmetric laser beam in cold underdense plasma, allowing for complete electron evacuation on the axis. Macchi *et al*. (2007) studied the propagation of an intense laser pulse in an underdense, inhomogeneous plasma on the time scale of several picoseconds. They addressed the effects of the ion dynamics following the charge-displacement self-channeling of the laser pulse. Pathak and Tripathi (2006) have studied nonlinear eigen mode of a plasma channel and examined its stability to stimulated Raman Scattering. However, the treatment is limited to intensities where electron hole is not created on the axis.

In this paper, we examine the issue of harmonic excitation of a self guided nonlinear laser eigen mode in a plasma, where complete electron evacuation occurs on the axis. Needless to mention, harmonic generation is one of the most dominating nonlinear effects induced by linearly polarized intense short pulse laser in a plasma. Third harmonic is particularly important as observed in several experiments (Lin *et al*., 2006; Kuo *et al*., 2007; Sunstov *et al*., 2010;

Address correspondence and reprint requests to: K.K. Magesh Kumar, Physics Department, Indian Institute of Technology Delhi, New Delhi-110016, India. E-mail: mageshkumar2006@gmail.com

Ganeev *et al.*, 2010; Yang *et al.*, 2003). Liu *et al.* (1993) have used the pump-probe technique to observe third harmonic generation in a preformed plasma. Nitikant and Sharma (2004) examined the resonant second-harmonic generation of a Gaussian laser short pulse undergoing periodic self-focusing in a preformed plasma. Ganeev *et al.* (2010) experimentally observed the third harmonic generation of picosecond and femtosecond laser pulses in plasma plumes. They showed that the technique can be used for generation of harmonics in the shorter wavelength range. Yang *et al.* (2003) have obtained an efficiency conversion greater than 0.1 percent of a strong third-harmonic emission from a plasma channel that is formed by self-guided propagation of femtosecond laser pulses in air. Similarly, Sunstov *et al.* (2010) studied the third-harmonic generation in air by a filamented femtosecond infrared laser pulse propagating through a thin plasma channel. Verma and Sharma (2009*a*; 2009*b*) have studied third harmonic generation by a finite spot size laser in a tunnel ionizing gas with density rising in a stepwise manner. Gupta *et al.* (2007) have investigated the generation of plasma wave and third harmonic generation at ultra relativistic laser power and obtained power of the third harmonic generation. Garg and Tripathi (2010) have studied resonant third harmonic generation in a semiconductor slab with density ripple of wave number q. Verma and Sharma (2011) obtained the mode structure of right circularly polarized nonlinear laser Eigen mode in a self created plasma channel in the presence of an axial magnetic field and Ghorbanalilu (2012) studied second and third harmonics generation in a strongly magnetized dense plasma.

Here we develop a two-dimensional slab model for nonlinear eigen mode of a ponderomotive force driven plasma channel, with perfect electron hole on the axis and study third harmonic generation of the eigen mode. The relativistic mass increase is self consistently incorporated while ions are taken to be immobile. In the axial region, the laser ponderomotive force exceeds ion space charge force on electrons, hence complete electron evacuation up to a width is obtained. Beyond this width, the ponderomotive force is balanced by space charge force. The relativistic mass nonlinearity adds to non-uniformity of the channel. The second harmonic component of ponderomotive force induces longitudinal oscillatory velocity on electrons and gives rise to second harmonic electron density perturbation. The latter couples with oscillatory velocity due to the laser to produce a nonlinear third harmonic current giving third harmonic radiation.

In Section 2, we study the mode structure of two-dimensional laser eigen mode in the self created plasma channel. In Section 3, we study the third harmonic generation of the self consistent laser eigen mode and estimate its efficiency. The results are discussed in Section 4.

2. NONLINEAR LASER EIGEN MODE

Consider a singly ionized cold collionless plasma of uniform electron density n_0^0. A two-dimensional intense short pulse laser propagates through it along $\hat{z}$ with fast phase variation as,

$$\mathbf{E} = \hat{y}A_T(x)e^{-i(\omega t - k_z z)}. \tag{1}$$

The duration of the pulse is larger than the electron plasma period but much shorter than the ion plasma period, so that the ions remain immobile. We look for a suitable profile of $A_T(x)$ that would propagate without convergence or divergence and allow A_T to acquire relativistically large values. The laser imparts oscillatory velocity to electrons, $\vec{v} = e\mathbf{E}/mi\omega\gamma$, where $\gamma = \sqrt{1 + a^2/2}$, $a = e|A_T|/m\omega c$, $-e$ and m are the electronic charge and rest mass, and c is the speed of light in vacuum. The laser exerts a ponderomotive force on electrons,

$$\mathbf{F_p} = e\nabla\phi_p, \tag{2}$$

where $\phi_p = -(mc^2/e)(\sqrt{1 + a^2/2} - 1)$. For an eigen mode, field amplitude does not change with z, hence the ponderomotive force has only $x-$ component. It pushes the electrons outward (to higher values of |x|) producing a space charge field $\mathbf{E_s} = -\nabla\phi_s$. The radial movement of electrons takes place as long as $\vec{F}_p > e\vec{E}_s$. On the time scale of a plasma period ω_p^{-1}, a quasi-steady state is reached when $\mathbf{F_p} = e\mathbf{E_s}$, or $\phi_s = -\phi_p$. From the Poisson's equation,

$$\nabla^2\phi_s = 4\pi e(n_e - n_0^0), \tag{3}$$

one may write, using $\phi_s = -\phi_p$, the modified electron density

$$n_e = n_0^0 - \frac{1}{4\pi e}\nabla^2\phi_p, \tag{4}$$

where n_0^0 is the ion density (equal to unperturbed electron density). Since, n_e cannot be negative, Eq. (4) is valid only as long as

$$n_0^0 > \frac{1}{4\pi e}\nabla^2\phi_p. \tag{5}$$

Thus, the electron density in the channel can be written as,

$$n_e = \begin{cases} 0 & \text{for } x < r_{0p} \\ n_0^0 - \frac{1}{4\pi e}\nabla^2\phi_p & \text{for } x > r_{0p} \end{cases}, \tag{6}$$

where r_{0p} is the value of x at which

$$\frac{\partial^2}{\partial x^2}\sqrt{1 + \frac{|E_y|^2 e^2}{2m^2\omega^2 c^2}}\Bigg|_{x = r_{0p}} = -\omega_p^2/c^2, \tag{7}$$

where $\omega_p = \sqrt{4\pi n_0^0 e^2/m} = k_p c$. One may note that the electron density increases from zero at |x| = r_{0p} to higher values as |x| increases.

https://doi.org/10.1017/S0263034612000985 Published online by Cambridge University Press

For $x < r_{0p}$ (for a symmetric mode), the laser field E_y may be written as,

$$E_y = A_0 cos(\alpha x) e^{-i(\omega t - k_z z)}, \tag{8}$$

where A_0 is the amplitude of the laser at $x = 0$ and $\alpha = \sqrt{(\omega^2/c^2) - k_z^2}$. For $x > r_{0p}$, E_y is governed by the wave equation

$$\frac{\partial^2}{\partial x^2} E_y + \left[\frac{\omega^2}{c^2}\left(1 - \frac{\omega_p^2}{\omega^2}\frac{n_e}{\gamma n_0^0}\right) - k_z^2\right] E_y = 0. \tag{9}$$

The term $\omega_p^2(ne/\gamma n_0^0)$ in the wave equation arises due to the contribution of current density, $\vec{J} = -n_e e \vec{v}$ driven by the laser pulse and $\vec{v}(= \hat{y} e E_y / m i \omega \gamma)$ is the oscillatory velocity imparted by the laser.

Using E_y from Eq. (1) in Eq. (9), writing $A_T = A\, e^{i\phi}$ with A and ϕ real, and separating out the real and imaginary parts of Eq. (9), we obtain

$$\frac{d}{dx}\left(A^2 \frac{d\phi}{dx}\right) = 0 \Rightarrow A^2 \frac{d\phi}{dx} = constant = C_1,$$

$$\frac{d^2 A}{dx^2} - \frac{C_1^2}{A^3} + \left[\frac{\omega^2}{c^2}\left(1 - \frac{\omega_p^2}{\omega^2}\frac{n_e}{\gamma n_0^0}\right) - k_z^2\right] A = 0. \tag{10}$$

One may multiply Eq. (10) by $e/m\omega c$ and write it for normalized amplitude $a = eA/m\omega c$ as,

$$\frac{d^2 a}{dx^2} - \frac{C_1^2}{a^3} + \left[\frac{\omega^2}{c^2}\left(1 - \frac{\omega_p^2}{\omega^2}\frac{n_e}{\gamma n_0}\right) - k_z^2\right] a = 0. \tag{11}$$

Using the value of n_e/n_0^0 from Eq. (4),

$$\frac{n_e}{n_0^0} = 1 + \frac{c^2}{2\omega_p^2}\left(\frac{a}{\sqrt{1 + a^2/2}}\frac{d^2 a}{dx^2} + \frac{1}{(1 + a^2/2)^{3/2}}\left(\frac{da}{dx}\right)^2\right), \tag{12}$$

Eq. (11) can be written as

$$\begin{aligned} &\frac{d^2 a}{dx^2} - \frac{C_1^2}{a^3}(1 + a^2/2) - \frac{a}{2(1 + a^2/2)}\left(\frac{da}{dx}\right)^2 \\ &+ \left[\frac{\omega^2}{c^2}\left(1 - \frac{\omega_p^2}{\omega^2\sqrt{1 + a^2/2}}\right) - \frac{k_z^2 c^2}{\omega^2}\right](1 + a^2/2) a = 0. \end{aligned} \tag{13}$$

As $x \rightarrow \infty$, the nonlinear terms vanish and $a \rightarrow 0$. The equation will remain well behaved only when $C_1 = 0$. At $x = r_{0p}$, $n_e/n_0^0 = 0$, Eq. (12) gives

$$\frac{d^2 a}{dx^2} = -\frac{2\sqrt{1 + a^2/2}}{a}\left[\frac{\omega_p^2}{c^2} + \frac{1}{2(1 + a^2/2)^{3/2}}\left(\frac{da}{dx}\right)^2\right], \tag{14}$$

while from Eq. (11), on putting $n_e/n_0^0 = 0$, and $C_1 = 0$, we get

$$\frac{d^2 a}{dx^2} = \left(\frac{\omega^2}{c^2} - k_z^2\right) a. \tag{15}$$

Comparing Eq. (14) and (15), we obtain,

$$\frac{1}{2(1 + a^2/2)^{3/2}}\left(\frac{da}{dx}\right)^2 = \left(\frac{\omega^2}{c^2} - k_z^2\right)\frac{a^2}{2\sqrt{1 + a^2/2}} - \frac{\omega_p^2}{c^2}. \tag{16}$$

We want a and da/dx to be continuous at $x = r_{0p}$, hence

$$\begin{aligned} a &= a_0 cos(\alpha r_{0p}), \\ \frac{da}{dx} &= -a_0 \alpha sin(\alpha r_{0p}). \end{aligned} \tag{17}$$

Using these in Eq. (16) we get an equation governing r_{0p},

$$\frac{a_0^2 \alpha^2 sin^2(\alpha r_{0p})}{2(1 + (a_0^2/2)(cos\alpha r_{0p})^2)^{3/2}} = \frac{(\omega^2/c^2 - k_z^2) a_0^2 cos^2 \alpha r_{0p}}{2\sqrt{1 + (a_0^2/2)(cos^2 \alpha r_{0p})}} - \frac{\omega_p^2}{c^2}, \tag{18}$$

One must choose $k_z < \omega/c$, ω_p to be small and a_0 such that the right hand side is +ve. Eq. (18) can be written as,

$$\frac{\alpha^2 c^2}{\omega^2} = \frac{2\omega_p^2}{\omega^2}\frac{\sqrt{1 + (a_0^2/2)cos^2(\alpha r_{0p})}}{a_0^2 cos^2(\alpha r_{0p})} + \frac{(\alpha^2 c^2/\omega^2) tan^2(\alpha r_{0p})}{1 + (a_0^2/2)(cos^2(\alpha r_{0p})}. \tag{19}$$

To obtain r_{0p} and α explicitly for a given ω_p/ω, we proceed as follows. At some large value of x we chose a small value of a. Now pick a value of ck_z/ω and take $da/dx = -\alpha' a$, where $\alpha' = (k_z^2 + (\omega_p^2/c^2) - (\omega^2/c^2))^{1/2}$. Solve Eq. (13) backward to smaller x, up to a point where $n_e = 0$, i.e., Eq. (16) is satisfied. Call this point $x = r_{0p}$. At this point, the continuity conditions (17) demand, $(1/a)(da/dx) = -\alpha tan(\alpha r_{0p})$. If this condition is not met, we try a different value of ck_z/ω and repeat the same procedure until this condition is satisfied. Once we get a suitable ck_z/ω and have r_{0p}, α, Eq. (19) gives the value of a_0.

We have plotted the hole half width of the electron (equivalent to hole radius) $r_{0p}\omega_p/c$ with a_0 in Figure 1 and ck_z/ω with a_0 in Figure 2. The hole radius increases rapidly with a_0 in the range of $a_0 \rightarrow$ 1–4 with a strong dependence on ω_p/ω and tends to saturate for larger values of a_0. With increase in ω_p/ω, the electron density on the shoulders of the channel increases resulting in considerable reduction in channel radius. From Figure 1 one may note that beyond a certain value of $a_0(= a_{min})$ the electrons are completely removed from the axis forming an electron hole. The value a_{min} increases with increase in ω/ω_p and electron evacuation does not occur for $a_{min} < 1$. With increase in laser amplitude, as the hole size increases, there is corresponding reduction in the phase velocity of the eigen mode (see Fig. 2). This is because the effective refractive index increases with increase in

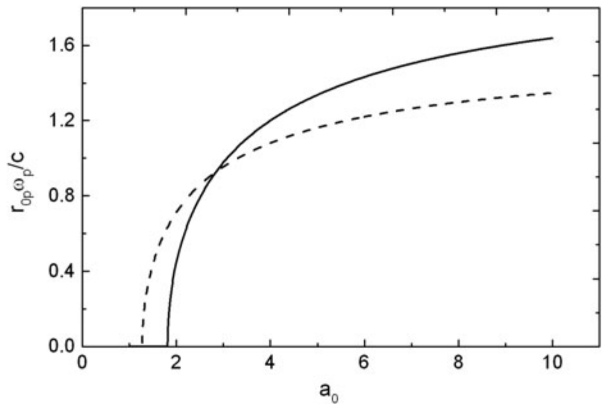

Fig. 1. Variation of normalized channel radius $r_{0p}\omega_p/c$ with laser amplitude a_0 for $\omega_p/\omega = 0.86$ (dot) and 0.83 (solid).

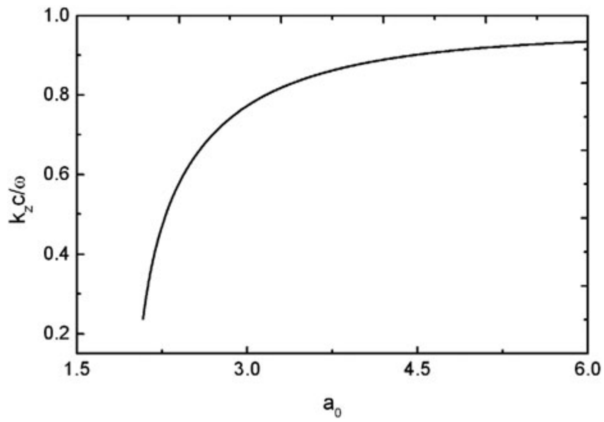

Fig. 2. Variation of k_zc/ω (inverse of phase velocity of eigen mode) with a_0 for $\omega/\omega_p = 1.2$.

laser amplitude a_0. The dispersion relation is plotted in Figure 3 for $a_0 = 2(dot)$, $3(solid)$. One may note that the eigen frequency shows a monotonous increase with wave vector of the mode with a strong dependence on a_0. For $\omega/\omega_p = 1.2$, $k_zc/\omega_p = 0.525$ and $a_0 = 2$, the phase velocity of the eigen mode turns out to be $\omega/k_zc = 2.25$ and the value

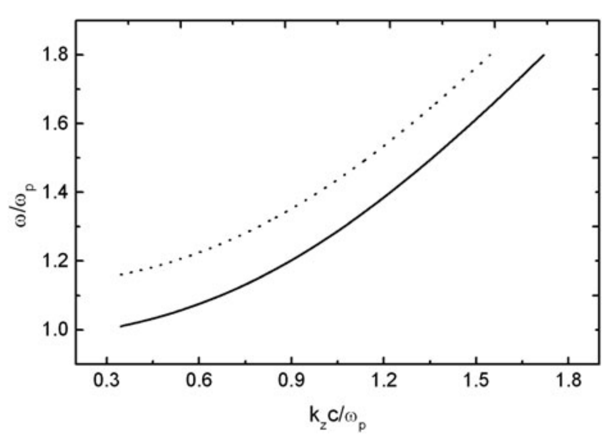

Fig. 3. Variation of ω/ω_p with k_zc/ω_p for $a_0 = 2$ (dot) and 3 (dash).

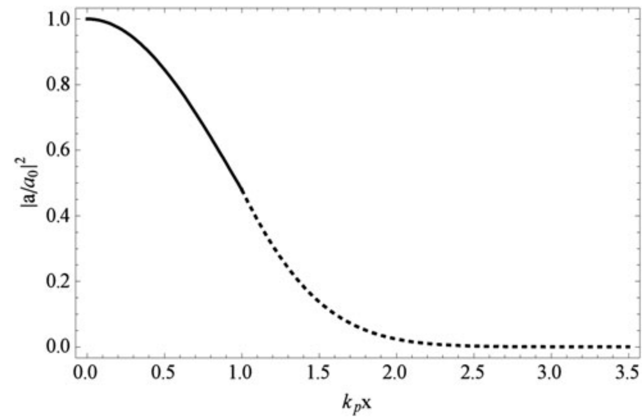

Fig. 4. Variation of $|a/a_0|^2$ with k_px for $a_0 = 2$, $\omega/\omega_p = 1.2$, $k_zc/\omega_p = 0.9$, and $k_pr_{0p} = 1$.

of ω/k_zc decreases with a_0 as mentioned earlier. Figure 4 shows the mode structure, $|a/a_0|^2$ versus normalized distance k_px, for $a_0 = 3$, $\omega/\omega_p = 1.2$, $k_zc/\omega_p = 0.9$ and $k_pr_{0p} = 1$. The eigen mode field varies cosinudally inside the channel (shown by solid line) and starts decaying from channel boundary (shown by dashed line) at $k_px = k_pr_{0p} = 1$. The mode intensity $|a/a_0|^2$ falls off to half of its axial value at $k_pr_{0p} = 1$. The intensity decreases more rapidly inside the electron hole and near the channel boundary. Outside the channel, it decreases slowly. The value of $|a|^2$ reduces to $1/10$ of its axial value at $k_px = 1.5$.

The power contained in the eigen mode per unit y width is,

$$P = \frac{m^2c^4\omega^2\epsilon_0}{2e^2}\int_0^\infty |a|^2dx. \tag{20}$$

where $|a|^2$ is the laser eigen mode intensity obtained by solving Eq. (13) as mentioned earlier. Multiplying both sides of Eq. (20) by c/ω_p, one obtains the normalized power,

$$\frac{Pc/\omega_p}{P_0} = \int_0^\infty |a|^2dx = \int_0^{r_{0p}} |a|^2dx + \int_{r_{0p}}^\infty |a|^2dx. \tag{21}$$

where $P_0 = (\omega^2/\omega_p^2)(m^2c^5\epsilon_0/2e^2) = 3.47(\omega/\omega_p)^2 \times 10^9 W$ and $x \to x\omega_p/c$. Figure 5 shows the variation of normalized power $(Pc/\omega_p)/P_0$ with a_0. The normalized power $(Pc/\omega_p)/P_0$ varies almost linearly with a_0. For $a_0 = 1.5$, $\omega_p/\omega = 0.83$, the power turns out to be $Pc/\omega_p = 1.6(\omega/\omega_p)^2 \times 10^{10} W$. Hence for $a_0 = 1.5$, the power obtained is slightly less than the critical power ($P_c = 1.78(\omega/\omega_p)^2 \times 10^{10} W$) needed for the formation of electron hole. Thus for the electrons to be completely removed from the axis, a_0 must be kept higher for the same value of ω_p/ω such that the condition $P/P_{cr} \geq 1$ is achieved. Increasing the value of a_0 from 2 to 5 the normalized power $(Pc/\omega_p)/P_0$ increases by a factor of 2. How ever with increase in ω_p/ω, $(Pc/\omega_p)/P_0$ decreases, so as r_{0p}. For $a_0 = 5$, $\omega_p/\omega = 0.83$ and $r_{0p} = 1.38c/\omega_p$, the normalized power $(Pc/\omega_p)/P_0$ turns out to be 9.0058, which is very close to

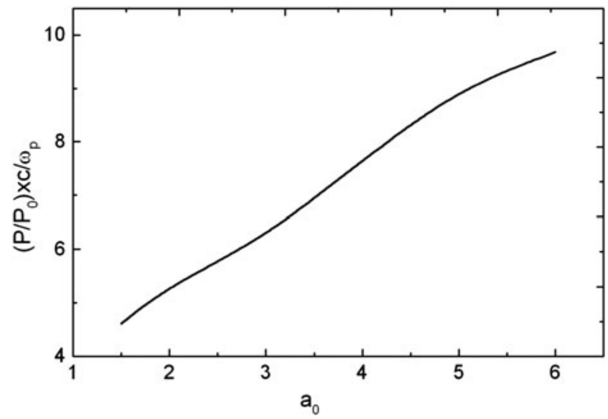

Fig. 5. Variation of the normalized power $(Pc/\omega p)/P_0$ with a_0 for $\omega/\omega_p = 1.2$ and $k_z c/\omega_p = 0.9$.

the value obtained by Sun *et al*. 1987. Hence, the power contained in the eigen mode for $a_0 = 5$ is $Pc/\omega_p = 3.948\left(\omega/\omega_p\right)^2 \times 10^{10} W$, exceeding the critical power P_{cr} by a factor of 2.

3. THIRD HARMONIC GENERATION

The laser eigen mode (E_y) propagating through the plasma channel with density profile given by Eq. (6) exerts a second harmonic ponderomotive force on electrons,

$$\mathbf{F}_{2\omega} = -(1/2)e\vec{\mathrm{v}} \times \mathbf{B} = -\hat{z}\frac{e^2 k_z E_y^2}{2mi\omega^2\gamma}. \quad (22)$$

Using this in the equations of motion and continuity one obtains the oscillatory velocity $\vec{v}_{2\omega}$ and density $n_{2\omega}$.

$$\vec{v}_{2\omega} = -\frac{\mathbf{F}_{2\omega}}{mi2\omega\gamma} = -\hat{z}\frac{e^2 k_z E_y^2}{4m^2\omega^3\gamma^2}, \quad (23)$$

$$n_{2\omega} = \frac{n_e k_z \mathrm{v}_z}{\omega} = -\frac{n_e e^2 k_z^2 E_y^2}{4m^2\omega^4\gamma^2}. \quad (24)$$

The density perturbation $n_{2\omega}$ couples with oscillatory velocity $\vec{v}$ to produce nonlinear current density at the third harmonic frequency (3ω),

$$\mathbf{J}^{NL} = -(1/2)n_{2\omega}e\vec{\mathrm{v}} = -\hat{y}\frac{\omega_p^2(n_e/n_0^0)k_z^2c^2}{8i\omega^4\gamma^2}a^2\omega\epsilon_0 E_y, \quad (25)$$

where $a = e|E_y|/m\omega c$. The nonlinear third harmonic current density produces third harmonic electric field $\mathbf{E}_{3\omega}$. This field produces self consistent current density $J_{3\omega}^L$,

$$\mathbf{J}_{3\omega}^L = i\frac{n_0^0 e^2 \mathbf{E}_{3\omega}}{3m\omega\gamma}. \quad (26)$$

The wave equation governing $\mathbf{E}_{3\omega}$ can be deduced from Maxwell's equations,

$$\nabla \times \mathbf{E}_{3\omega} = 3i\omega\mathbf{B}_{3\omega}, \quad (27)$$

$$\nabla \times \mathbf{B}_{3\omega} = -3i\omega\mu_0(\mathbf{J}^{NL} + \mathbf{J}_{3\omega}^L) - i\frac{3\omega}{c^2}\mathbf{E}_{3\omega}. \quad (28)$$

Since $\boldsymbol{J}^{NL}$ is parallel to $\hat{y}$ (cf. Eq. (25)), $\mathbf{E}_{3\omega}$ is also parallel to $\hat{y}$. Defining $a_{3\omega} = e\,E_{3\omega y}/m\omega c$ and taking fast t,z variation as $e_z^{-i(3\omega t - k_{3z}z)}$, we obtain from Eqs. (25)–(28),

$$\frac{d^2 a_{3\omega}}{dx^2} + 2ik_{3z}\frac{\partial a_{3\omega}}{\partial z} + \left(\frac{9\omega^2}{c^2} - \frac{\omega_p^2(n_e/n_0^0)}{c^2\gamma} - k_{3z}^2\right)\times a_{3\omega} = \frac{3}{8}a^3(k_z c/\omega)^2\frac{\omega_p^2(n_e/n_0^0)}{\gamma^2 c^2}. \quad (29)$$

One may note that the nonlinear third harmonic source current density is finite only in the outer region $|x| > r_{0p}$. It excites a number of eigen modes in the channel at the third harmonic. We consider the excitation of the fundamental mode of the third harmonic that has the mode structure similar to that of the pump laser,

$$a_{3\omega} = eE_{3\omega y}/m\omega c = A_{3\omega}(z)F(x)e^{-i(3\omega t - k_{3z}z)}, \quad (30)$$

$$F(x) = \begin{cases} a_0 cos(\alpha x) & \text{for } 0 < |x| < r_{0p} \\ a(x) & \text{for } |x| > r_{0p} \end{cases}. \quad (31)$$

where $k_{3z} = \sqrt{\frac{9\omega^2}{c^2} - \alpha^2}$.

Substituting Eq. (30) in (29), multiplying the resulting equation by $F(x)^* dx$ and integrating from $-\infty$ to ∞, we obtain,

$$\frac{\partial A_{3\omega}}{\partial z} - i\beta A_{3\omega} = \frac{3}{16ik_{3z}}\left(\frac{k_z c}{\omega}\right)^2\frac{\omega_p^2}{c^2}Ge^{-i(3k_z - k_{3z})z}, \quad (32)$$

where $\beta = \frac{1}{2k_{3z}}\left[\frac{8\omega^2}{c^2} + k_z^2 - k_{3z}^2\right]$, $G = \frac{\int_{-\infty}^{\infty} a^3(x)((ne/n_0^0)/\gamma^2)F(x)^* dx}{\int_{-\infty}^{\infty}|F(x)|^2 dx}$.

Effectively the integral in the numerator of G is the sum of two integrals one with limits $-\infty$ to $-r_{0p}$ and then from r_{0p} to ∞ as there are no electrons ($n_e = 0$) in the inner region. One may solve Eq. (32) on taking $\partial/\partial z = -i\delta$, $\delta = (3k_z - k_{3z})$. Hence,

$$A_{3\omega}(z) = \frac{3(k_z c/\omega)^2 G e^{-i(\beta + 3k_z - k_{3z})z}}{16[8(\omega/\omega_p)^2 + (k_z c/\omega_p)^2 - 3(k_{3z}c/\omega_p)^2 + (6k_{3z}c/\omega_p)(k_z c/\omega_p)]}, \quad (33)$$

$$\left|\frac{a_{3\omega}}{a_0}\right|^2 = \left(\frac{3(k_z c/\omega)^2 G}{16[8(\omega/\omega_p)^2 + (k_z c/\omega_p)^2 - 3(k_{3z}c/\omega_p)^2 + (6k_{3z}c/\omega_p)(k_z c/\omega_p)]}\right)^2. \quad (34)$$

In the fundamental mode, the amplitude of the third harmonic is maximum at the channel axis. The efficiency of the third harmonic shows a strong relationship with laser amplitude a_0 and

https://doi.org/10.1017/S0263034612000985 Published online by Cambridge University Press

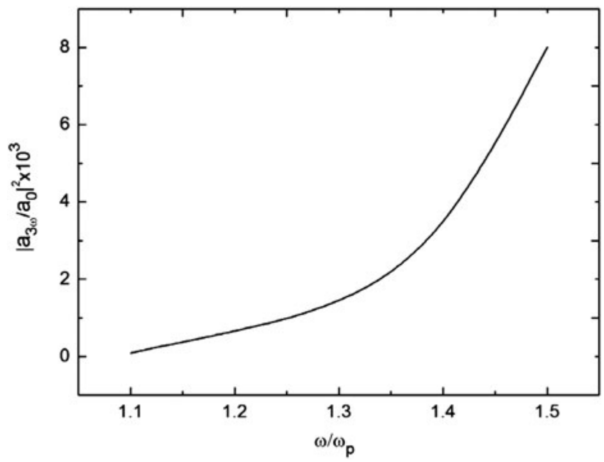

Fig. 6. Variation of the square of normalized third harmonic amplitude $|a_{3\omega}/a_0|^2$ with ω/ω_p for $a_0 = 3$.

frequency ω. Figure 6 shows the variation of axial amplitude of the third harmonic with normalized laser frequency ω/ω_p for $a_0 = 3$. With increase in normalized laser frequency ω/ω_p the fundamental and third harmonic wave vectors $k_z c/\omega_p$, $k_{3z}c/\omega_p(\approx 3\omega/\omega_p)$ and inverse of the phase velocity $k_z c/\omega$ increases. Hence the denominator in Eq. (34) decreases steadily, whereas the numerator monotonously increases with ω/ω_p. The third harmonic efficiency $|a_{3\ \omega}/a_0|^2$ at constant a_0 shows a gradual increase in the range of $\omega/\omega \rightarrow 1.1$–$1.3$ and increases bit faster beyond $\omega/\omega_p = 1.3$. Beyond $\omega/\omega_p = 1.3$ the denominator in Eq. (34) attains a fairly constant value.

From Figure 7 one may note that the efficiency gradually increases with the laser amplitude a_0 for $\omega/\omega_p = 1.2$. However with the increase in a_0, the cavitation radius r_{0p} increases and increasing r_{0p} adversely effects the growth of third harmonic efficiency $|a_{3\omega}/a_0|^2$. But the laser intensity amplitude a_0^2 is predominant both inside and outside the channel. Hence with increase in the laser amplitude a_0 the lowering of third harmonic efficiency due to increasing r_{0p} can be compensated. However beyond $a_0 = 3$, the channel radius r_{0p} tends to saturate and the third harmonic efficiency grows with a_0.

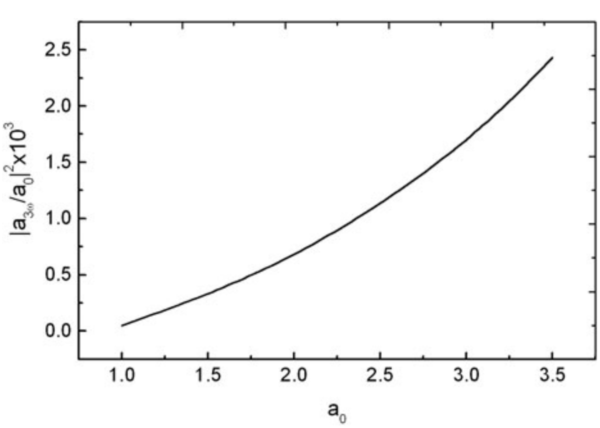

Fig. 7. Variation of the square of normalized third harmonic amplitude $|a_{3\omega}/a_0|^2$ with a_0 for $\omega/\omega_p = 1.2$ and $k_z c/\omega_p = 0.9$.

To validate the efficacy of our analytical calculation we compare our results with the experimental results obtained by Kuo *et al.* (2007). Kuo *et al.* (2007) have experimentally demonstrated the enhancement of relativistic third-harmonic generation in both uniform and rippled density plasma waveguide using linearly polarized laser beam of amplitude $a_0 = 1$. For the axially uniform channel case, they have obtained an efficiency of 1.1×10^{-8} at plasma density $n_0^0 = 4.8\times 10^{18}\ cm^{-3}$. For a comparison, we may calculate the conversion efficiency from Eq. (31) for the parameters: $\omega_p/\omega 0.05$ (corresponding to $n_0^0 = 4.8\times10^{18}\ cm^{-3}$ at $1\mu m$ laser wavelength) and $a_0 = 1.5$. The conversion efficiency $|a_{3\omega}/a_0|^2$ of third harmonic for the aforementioned parameters turns out to be 1.95×10^{-8}, which are within a factor of 2 from Kuo *et al.* (2007). However the efficiency of the third harmonic can be improved by increasing the laser frequency or by increasing the laser amplitude a_0 as shown in Figures 6 and 7.

4. CONCLUSIONS

A self consistent non-paraxial formalism of laser guiding in a self created channel with a perfect hole in the interior, developed here reveals that inside the hole, in two dimensions, the laser field is sinusoidal in x while its amplitude falls off with x beyond $x = r_{0p}$. The radius of the hole r_{0p} increases with normalized laser amplitude and tends to saturate for large values of a_0. The frequency of the eigenmode ω increases with wave vector k_z with a strong dependence on laser amplitude a_0. The power contained in the laser eigen mode is found to vary almost linearly with a_0

The laser eigen mode produces linearly polarized third harmonic outside and inside the electron cavity. The conversion efficiency of the laser eigen mode into the fundamental radial eigen mode of the third harmonic $|a_{3\ \omega}/a_0|^2$ shows a gradual increases as ω/ω_p increases from 1.1 to 1.3 and sharply increases beyond $\omega/\omega_p = 1.3$. The third harmonic conversion efficiency increases with a_0 more than linearly. For the parameters of the experiment by (Kuo *et al.*, 2007) the conversion efficiency in a unrippled plasma calculated by our model is in reasonable agreement with the experimental result.

ACKNOWLEDGEMENT

One of the authors, Magesh would like to thank IIT Delhi for financial support.

REFERENCES

Borisov, A.B., Borovskiy, A.V., Shiryaev, O.B., Korobkin, V.V., Prokhorov, A.M., Solem, J.C., Luk, T.S., Boyer, K. & Rhodes, C.K. (1992). Relativistic and charge-displacement self-channeling of intense ultrashort laser pulses in plasmas. *Phys. Rev. A* **45**, 5830–5845.

Bulanov, S.V., Pegoraro, F. & Pukhov, A.M. (1995). Two-dimensional regimes of self-focusing, wake field generation, and induced focusing of a short intense laser pulse in an underdense plasma. *Phys. Rev. Lett*. **74**, 710–713.

Burnett, N.H. & Enright, G.D. (1990). Population inversion in the recombination of optically-ionized plasmas. *IEEE J. Quant. Electron*. **26**, 1797–1808.

Durfee Iii, C.G. & Milchberg, H.M. (1993). Light pipe for high intensity laser pulses. *Phys. Rev. Lett*. **71**, 2409–2412.

Ehrlich, Y., Cohen, C., Zigler, A., Krall, J., Sprangle, P. & Esarey, E. (1996). Guiding of High Intensity Laser Pulses in Straight and Curved Plasma Channel Experiments. *Phys. Rev. Lett*. **77**, 4186–4189.

Ganeev, R.A., Boltaev, G.S., Tugushev, R.I., Usmanov, T., Baba, M. & Kuroda, H. (2010). Third harmonic generation in plasma plumes using picosecond and femtosecond laser pulses. *J. Opt*. **12**, 1–7.

Garg, V. & Tripathi, V.K. (2010). Resonant third harmonic generation of an infrared laser in a semiconductor wave guide. *Laser Part. Beams* **28**, 327–332.

Geddes, C.G.R., Toth, C.S., Tilborg, J.V., Esarey, E., Schroeder, C.B., Cary, J. & Lee-Mans, W.P. (2005). Guiding of Relativistic Laser Pulses by Preformed Plasma Channels. *Phys. Rev. Lett*. **95**, 145002–145006.

Ghorbanalilu, M. (2012). Second and third harmonics generation in the interaction of strongly magnetized dense plasma with an intense laser beam. *Laser Part. Beams* **30**, 291–298.

Gupta, M.K., Sharma, R.P. & Mahmoud, S.T. (2007). Generation of plasma wave and third harmonic generation at ultra relativistic laser power. *Laser Part. Beams* **25**, 211–218.

Jackel, S., Burris, R., Grun, J., Ting, A., Manka, C., Evans, K. & Kosakowskii, J. (1995). Channeling of terawatt laser pulses by use of hollow waveguides. *Opt. Lett*. **20**, 1086–1088.

Kumarappan, V., Kim, K.Y. & Milchberg, H.M. (2005). Guiding of intense laser pulses in plasma waveguides produced from efficient, femtosecond end-pumped heating of clustered gases. *Phys. Rev. Lett*. **94**, 205004–205008.

Kuo, C.C., Pai, C.H., Lin, M.W., Lee, K.H., Lin, J.Y., Wang, J. & Chen, S.Y. (2007). Enhancement of relativistic harmonic generation by an optically preformed periodic plasma waveguide. *Phys. Rev. Lett*. **98**, 033901–033903.

Lin, M.W., Chen, Y.M., Pai, C.H., Kuo, C.C. Lee, K.H., Wang, J., Chen, S.Y. & Lin, J.Y. (2006). Programmable fabrication of spatial structures in a gas jet by laser machining with a spatial light modulator. *Phys. Plasmas* **13**, 110701–110704.

Liu, X., Umstadter, D., Esarey, E. & Ting, A. (1993). *IEEE Trans. Plasma Sci*. **21**, 90.

Macchi, A., Bigongiari, A., Ceccherini, F., Cornolti, F., Liseikina, T.V., Borghesi, M., Kar, S. & Romagnani, L. (2007). Ion dynamics and coherent structure formation following laser pulse self-channeling. *Plasma Phys. Contr. Fusion* **49**, 71–78.

Malka, V., Faure, J., Marques, J.R., Amiranoff, F., Courtois, C., Najmudin, Z., Krushenick, K., Salvati, M.R. & Modena, A., Najmudin, Z., Dangor, A.E., Clayton, C.E., Marsh, K.A. Joshi, C., Malka, V., Darrow, C.B., Danson, C., Neely, D. & Walsh, F.N. (1995). Electron acceleration from the breaking of relativistic plasma waves. *Nat. (London)* **377**, 606–608.

Modena, A., Najmudin, Z., Dangor, A.E., Clayton, C.E., Marsh, K.A., Joshi, C.,Malka, V., Darrow, C.B., Danson, C., Neely, D. & Walsh, F.N. (1995). Electron acceleration from the breaking of relativistic plasma waves. *Nat*. **377**, 606–608.

Mora, P. & Antonsen, Jr., T.M. (1996). Electron cavitation and acceleration in the wake of an ultraintense, self-focused laser pulse. *Phys. Rev. E* **53**, 2068–2071.

Nikitin, S.P., Antonsen, T.M., Clark, T.R., Li, Y. & Milchberg, H.M. (1997). Guiding of intense femtosecond pulses in preformed plasma channels. *Opt. Lett*. **22**, 1787–1789.

Nitikan, S.P. & Sharma, A.K. (2004). Resonant second-harmonic generation of a short pulse laser in a plasma channel. *J. Phys. D: Appl. Phys*. **37**, 2395–2398.

Pathak, V.B. & Tripathi, V.K. (2006). Nonlinear electromagnetic plasma eigenmodes and their stability to stimulated Raman scattering. *Phys. Plasmas* **13**, 082105–082108.

Sarkisov, G.S., Bychenkov, V.Yu., Novikov, V.N. & Tikhonchuk, V.T., Maksimchuk, A., Chen, S.Y., Wagner, R., Mourou, G. & Umstadter, G. (1996). Self-focusing, channel formation, and high-energy ion generation in interaction of an intense short laser pulse with a He jet. *Phys. Rev. E* **59**, 7042–7054.

Singh, A & Singh, N. (2011). Relativistic guidance of an intense laser beam through an axially non-uniform plasma channel. *Laser Part. Beams* **29**, 291–298.

Sprangle, P., Esarey, E., Krall, J. & Joyce, G. (1992). Propagation and guiding of intense laser pulses in plasmas. *Phys. Rev. Lett*. **69**, 2200–2203.

Sprangle, P., Esarey, E., Ting, A. & Joyce, G. (1988). Laser wake_eld acceleration and relativistic optical guiding. *Appl. Phys. Lett*. **53**, 2146–2148.

Sun, G., Edward, O., Lee, Y.C. & Guzdar, P. (1987). Self-focusing of short intense pulses in plasmas. *Phys. Fluids* **30**, 526–532.

Suntsov, S., Abdollahpour, D., Papazoglou, D.G. & Tzortzakis, S. (2010). Filamentation-induced third-harmonic generation in air via plasma-enhanced third-order susceptibility. *Phys. Rev. A* **81**, 033817–033820.

Tabak, M., Hammer, J., Glinsky, M.E., Kruer, W.L., Wilks, S.C., Wood worth, J., Campbell, E.M., Perry, M.D. & Mason, R.J. (1994). Ignition and high gain with ultrapowerful lasers. *Phys. Plasmas* **1**, 1626–1634.

Tajima, T. & Dawson, J.M. (1979). Laser electron accelerator. *Phys. Rev. Lett*. **43**, 267–270.

Ting, A., Moore, C.I., Krushelnick, K. Manka, C., Esarey, E. Sprangle, P., Hubbard, R., Burris, H.R., Fischer, R. & Baine, M. (1997). Plasma wakefield generation and electron acceleration in a self-modulated laser wakefield accelerator experiment. *Phys. Plasmas* **4**, 1889–1899.

Verma, U. & Sharma, A.K. (2009*a*). Effect of laser self defocusing on third harmonic generation in a tunnel ionizing gas. *Phys. Plasmas* **16**, 013101–013105.

Verma, U. & Sharma, A.K. (2009*b*). Effect of self focusing on the prolongation of laser produced plasma channel. *Laser Part. Beams* **27**, 33–39.

Verma, U. & Sharma, A.K. (2011). Nonlinear electromagnetic Eigen modes of a self created magnetized plasma channel and its stimulated Raman scattering. *Laser Part. Beams* **29**, 471–477.

Yang, H., Zhang, J., Zhang, J., Zhao, L.Z., Li, Y.J., Teng, H., Li, Y.T., Wang, Z.H., Chen, Z.L., Wei, Z.Y., Ma, J.X., Yu, W. & Sheng, Z.M. (2003). Third-order harmonic generation by self-guided femtosecond pulses in air. *Phys. Rev. E* **67**, 015401–015403.